Interaction between mixed-valent rare-earth impurities in BCS superconductors

Ke-qi Luo and Jun Li
Department of Physics, Nanjing University, Nanjing 210008, People's Republic of China

Chang-de Gong
Chinese Center of Advanced Science and Technology (World Laboratory), P.O. Box 8703, Beijing 100080, China
and Micro-Structure Laboratory of Solid State Physics, Nanjing University, Nanjing 210008, People's Republic of China
(Received 19 January 1994)

The Goldstone-Feynman diagrammatic technique is adopted to study the interaction between mixed-valent rare-earth impurities in BCS superconductors. The influence of cerium-impurity coupling together with isolated cerium-impurity upon superconductivity of $Th_{1-x}Ce_x$ system is worked out. In comparison with magnetic rare-earth impurities, depression of superconductivity due to impurity interaction of nonmagnetic mixed-valent rare-earth dopants is much smaller.

I. INTRODUCTION

Rare-earth ions doped in conventional metals and superconductors can behave either as magnetic or nonmagnetic impurities due to various interactions between the isolated dopants and electrons in the host. Furthermore, the exchange interaction between the doped ions themselves mediated by host electrons can play an important role in the case of magnetic impurities.[1-6] For example, the reentrant behavior of superconductivity in $La_{0.75}Th_{0.25}Ce_x$,[4] and the enhanced superconductivity in Co_xNbSe_2;[4] unsolved by Abrikosov-Gorkov theory,[3] would remain unexplained until the consideration of the influence of Ruderman-Kittel-Kasuya-Yosida (RKKY) coupling on superconductivity.

In this paper, we will discuss the case of nonmagnetic impurities, i.e., the mixed-valent rare-earth system such as $Th_{1-x}Ce_x$.[7,8] Generally, cerium may have two different ionic configurations: (i) $Ce^{3+}(4f^1)$ with energy level E_1 and angular momentum $J=\frac{5}{2}$ and (ii) $Ce^{4+}(4f^0)$ with energy level E_0 and angular momentum $J=0$. For isolated ion of cerium, $E_1<E_0$, so that $4f^1$ configuration is ground state and Ce^{3+} shows large magnetic moment. However, in alloys like $Th_{1-x}Ce_x$, the energy levels of the two configurations $4f^0$ and $4f^1$ are shifted as $E_0\rightarrow E_0+\tilde{E}_0$, $E_1\rightarrow E_1+\tilde{E}_1$ due to the mixing interaction between the cerium $4f$ electrons and the host conducting electrons. In this way, the valence of doped cerium ions is neither three (Ce^{3+}) nor four (Ce^{4+}), and in strong mixing coupling or large N ($N=2J+1$) limit, the two energy levels are reversed as $E_1+\tilde{E}_1>E_0+\tilde{E}_0$. The averaged valence of cerium impurity lies between three and four. The suppression of superconductivity due to isolated mixed-valent rare-earth impurities has been discussed by using mixed Goldstone-Feynman technique.[9-12] It is an interesting problem to elucidate the role of interimpurity correlation in this kind of alloys in comparison with that of the RKKY interaction as mentioned above. We will extend the Goldstone-Feynman diagrammatic technique[11-15] to include impurity-impurity coupling on a single Goldstone time axis and work out the concentration dependence of superconducting transition temperature $T_c(x)$.

II. FREE-ENERGY DENSITY

The total Hamiltonian of superconducting $Th_{1-x}Ce_x$ system can be written as[11,12]

$$
\begin{aligned}
H&=H_0+H' ,\\
H_0&=\sum_j [E_0X_{00}^{(j)}+\sum_m E_1X_{mm}^{(j)}]\\
&\quad+\sum_k \xi_k(a_k^+a_k+a_{-k}^+a_{-k})\\
&\quad+(-\Delta)\sum_k (a_k^+a_{-k}^++a_{-k}a_k) ,\\
H'&=\frac{1}{\sqrt{N}}\sum_j\sum_{km}[(V_ka_k^+X_{0m}^{(j)}+\text{H.c.})\\
&\quad+(V_{-k}a_{-k}^+X_{0m}^{(j)}+\text{H.c.})] ,
\end{aligned}
\tag{2.1}
$$

where j represents lattice sites, k stands for $k\uparrow$, $-k$ stands for $-k\downarrow$, $X_{ml}=|m\rangle\langle l|$ are the Hubbard projection operators, H' is the Hamiltonian of mixing interaction between electron of extended states and $4f$ electron, and E_0,E_1 are energy levels of $4f^0,4f^1$ configurations of a single cerium ion, respectively. By extending the perturbation H', partition function of the system may be written in the form of[11,12]

$$
\frac{Z}{Z_0}=\sum_{j_1}\sum_{j_2}\cdots\sum_{j_{2n}}\sum_{n=0}^{\infty}(-1)^n\int_0^\beta d\tau_1\int_0^{\tau_1}d\tau_2\cdots\int_0^{\tau_{2n-1}}d\tau_{2n}\langle h'_{j_1}(\tau_1)h'_{j_2}(\tau_2)\cdots h'_{j_{2n}}(\tau_{2n})\rangle ,
\tag{2.2}
$$

where Z_0 represents the partition function of pure superconductor, and h' is the mixing interaction Hamiltonian of single-impurity problem. Up to higher-order approximation of two-impurity coupling, we may have[9,10]

$$\frac{Z}{Z_0}=1+\sum_j S_j+\sum_{\{j_1 j_2\}}(S_{j_1}S_{j_2}+S_{j_1 j_2})$$
$$=\prod_j(1+S_j)\left[1+\sum_{\{j_1 j_2\}}\tilde{S}_{j_1 j_2}\right], \quad (2.3)$$

where $S_j, S_{j_1 j_2}$ represent contribution of single impurity and coupling of two impurities to the partition function of the system, respectively, and $\tilde{S}_{j_1 j_2}=S_{j_1 j_2}/[(1+S_{j_1})(1+S_{j_2})]$ is a renormalized one of the impurity coupling term to the partition function.

If impurity concentration x is very low ($x<<1$), impurities in the system are nearly independent, coupling between impurities could be neglected. In this case it is sufficient to consider only the influence of isolated single impurities; when x increases, the impurity coupling is enhanced and its influence upon superconductivity should be included.

According to the study of single impurity behavior, we may have the relation[11,12]

$$\prod_j(1+S_j)=\left[\sum_m \exp[-\beta(E_m+\tilde{E}_m)]\right]^{N_i}, \quad (2.4)$$

where N_i denotes the impurity numbers, E_m are energy levels of $4f$ configurations, and $E_m+\tilde{E}_m$ are shifted energies owing to the mixing interaction between extending electrons and $4f$ electrons. For large N limit, $\tilde{E}_0$, $\tilde{E}_1$ may be expressed as following in terms of Brillouin-Wigner theory[11,12]

$$\tilde{E}_0=N\rho V^2\left[-\ln\left[\frac{\beta D}{2\pi}\right]+\mathrm{Re}\psi\left[\frac{1}{2}+i\beta\frac{|\tilde{E}_0-E_f|}{2\pi}\right]\right], \quad (2.5a)$$

$$\tilde{E}_1=\rho V^2\left[-\ln\left[\frac{\beta D}{2\pi}\right]+\mathrm{Re}\psi\left[\frac{1}{2}+i\beta\frac{|\tilde{E}_1+E_f|}{2\pi}\right]\right], \quad (2.5b)$$

where D is the half bandwidth of extending electron, $E_f=E_1-E_0$, $\psi(x)=(d/dx)\ln\Gamma(x)$, and $\Gamma(x)$ is gamma function. From formulas (2.3) and (2.4) mentioned above, the free-energy density of the system can be obtained as

$$f=f_0-x\beta^{-1}\ln\left[\sum_m e^{-\beta(E_m+\tilde{E}_m)}\right]$$
$$-\frac{\beta^{-1}}{N}\ln\left[1+\sum_{\{j_1 j_2\}}\tilde{S}_{j_1 j_2}\right]$$
$$=f_0-x\beta^{-1}\ln\left[\sum_m e^{-\beta(E_m+\tilde{E}_m)}\right]$$
$$+\frac{1}{N}\sum_{\{j_1 j_2\}}F_{j_1 j_2}(|\mathbf{R}_{j_1}-\mathbf{R}_{j_2}|)$$

where $F_{j_1 j_2}(|\mathbf{R}_{j_1}-\mathbf{R}_{j_2}|)$ represents the free energy of the impurity coupling. The nearest-neighbor approximation is adopted for the last term including $F_{j_1 j_2}(\mathbf{R})$ in the expression above, thus leading to

$$f=f_0-x\beta^{-1}\ln\left[\sum_m e^{-\beta(E_m+\tilde{E}_m)}\right]+x^2 m_i F_{j_1 j_2}(\bar{R}), \quad (2.6)$$

where $\bar{R}$ indicates the average distance of the nearest-neighbor impurities, m_i is the numbers of the nearest impurity.

Now, we investigate the free energy of impurity coupling. Along one time axis $(0,\beta)$, the generators of mixed Goldstone-Feynman impurity-coupling diagrams are shown in Fig. 1.[11,12]

All impurity coupling diagrams can be generated from Fig. 1, by exchanging impurity position $\mathbf{R}_1$ and $\mathbf{R}_2$, and exchanging their occupied probabilities of initial state P_0 and final state P_m, respectively. Thus yield 24 impurity coupling diagrams, which are divided into 6 rotation classes.[11,12]

Owing to exchanging interaction between extending electron and $4f$ electron, in terms of Brillouin-Wigner theory, the occupancies of the $4f$ configurations can be found as $P_0\sim 1$, $P_m\sim 0$,[11,12] and, as a result, of all 24 coupling diagrams only 6 diagrams shown in Fig. 2 are able to make contributions to the free energy in the low-temperature limit.

The free energies from the impurity-correlation diagrams (Fig. 2) can be written as following in terms of the diagrammatic rules of mixed Goldstone-Feynman coupling diagram on a single time axis (see Appendix A)

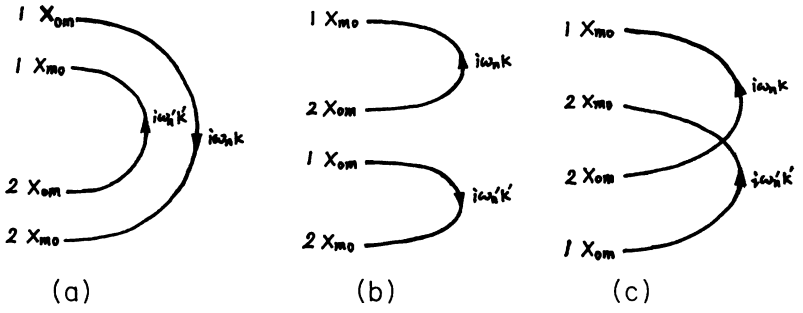

FIG. 1. Generators of the mixed Goldstone-Feynman diagrams of two impurity coupling on one time axis $(0,\beta)$.

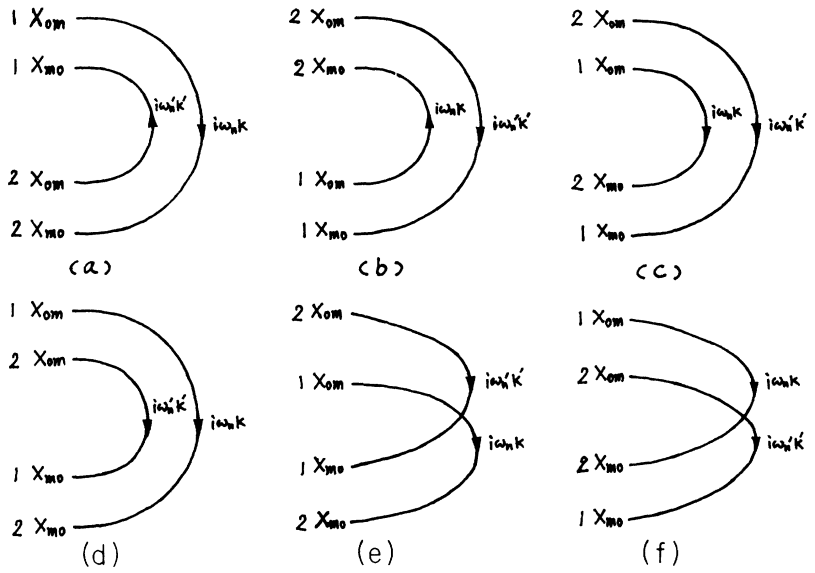

FIG. 2. Six reserved coupling diagrams, which are able to make a contribution to the partition function of the system.

$$F_{ab}=\text{Fig. 2(a)}+\text{Fig. 2(b)}=\beta^{-1}\tilde{P}_0\tilde{P}_0\left[\sum_{\omega_n}\sum_{\omega_n'}\frac{g(\mathbf{R}_1-\mathbf{R}_2,i\omega_n)g(\mathbf{R}_1-\mathbf{R}_2,i\omega_n')}{\beta(i\omega_n-\epsilon_1)(i\omega_n'-\epsilon_1)}\left[\frac{1}{i\omega_n-\epsilon_1}+\frac{1}{i\omega_n'-\epsilon_1}\right]+\sum_{\omega_n}\frac{g^2(\mathbf{R}_1-\mathbf{R}_2,i\omega_n)}{(i\omega_n-\epsilon_1)^2}\right], \tag{2.7a}$$

$$F_{cd}=\text{Fig. 2(c)}+\text{Fig. 2(d)}=\beta^{-1}\tilde{P}_0\tilde{P}_0\left\{\sum_{\omega_n}\sum_{\omega_n'}\frac{g(\mathbf{R}_1-\mathbf{R}_2,i\omega_n)g(\mathbf{R}_1-\mathbf{R}_2,i\omega_n')}{\beta(i\omega_n+i\omega_n'-2\epsilon_1)}\left[\frac{1}{(i\omega_n-\epsilon_1)^2}+\frac{1}{(i\omega_n'-\epsilon_1)^2}\right]\right\}, \tag{2.7b}$$

$$F_{ef}=\text{Fig. 2(e)}+\text{Fig. 2(f)}=\beta^{-1}\tilde{P}_0\tilde{P}_0\left[\sum_{\omega_n}\sum_{\omega_n'}\frac{2g(\mathbf{R}_1-\mathbf{R}_2,i\omega_n)g(\mathbf{R}_1-\mathbf{R}_2,i\omega_n')}{\beta(i\omega_n-\epsilon_1)(i\omega_n'-\epsilon_1)(i\omega_n+i\omega_n'-2\epsilon_1)}+\sum_{\omega_n}\frac{-g^2(\mathbf{R}_1-\mathbf{R}_2,i\omega_n)}{\beta(i\omega_n-\epsilon_1)^3}\right], \tag{2.7c}$$

where $\epsilon_1=E_1+\tilde{E}_1-(E_0+\tilde{E}_0)$, is the difference of the shifted energy levels between the $4f^1$ and $4f^0$ configuration, $g(\mathbf{R}_1-\mathbf{R}_2,i\omega_n)$ is the intersite Green's function of superconducting electron. We can express $g(\mathbf{R}_1-\mathbf{R}_2,i\omega_n)$ in the form of (see Appendix B)

$$\begin{aligned}g(\mathbf{R}_1-\mathbf{R}_2,i\omega_n)&=\frac{1}{N}\sum_{km\sigma}|V_{km\sigma}|^2e^{-i\mathbf{k}\cdot(\mathbf{R}_1-\mathbf{R}_2)}\left[\frac{u_k^2}{i\omega_n-E_k}+\frac{v_k^2}{i\omega_n+E_k}\right]\\&=-\frac{\Gamma}{\alpha}e^{-(\alpha\beta/2y)\sqrt{\Delta^2+\omega_n^2}}\left[\frac{\sqrt{\Delta^2+\omega_n^2}\cos\alpha+i\omega_n\sin\alpha}{\sqrt{\Delta^2+\omega_n^2}}\right]\end{aligned} \tag{2.8}$$

where $\alpha=k_f|\mathbf{R}_1-\mathbf{R}_2|$, $\Gamma=\langle|V_{km\sigma}|^2\rangle$ is the orientative average value of $|V_{km\sigma}|^2$ in momentum space near the Fermi surface, $u_k^2=\frac{1}{2}(1+\xi_k/E_k)$, $v_k^2=\frac{1}{2}(1-\xi_k/E_k)$, $E_k=\sqrt{\Delta^2+\xi_k^2}$, and Δ is the energy gap.

III. DEPRESSION OF T_c

By the way of calculating minimum value of the free energy density (2.6), T_c equation for the $Th_{1-x}Ce_x$ superconductive system can be derived as

$$\rho\left[\ln\frac{T_c}{T_{c0}}+A(x,T_c)\right]+x^2m\left.\frac{\partial F_{12}(\bar{R})}{\partial\Delta^2}\right|_{\Delta^2=0}=0, \tag{3.1}$$

where[11,12]

TABLE I. Physical parameters in the paper.

$r=\rho(u)V^2$ $=\pi\Gamma$ (eV)	$E_f(r)$	U (eV)	$\rho(u)$	n_f	$\tilde{E}_0$ (eV)	$\tilde{E}_1$ (eV)
0.031	−1.71	∞	0.67	0.43	−0.30	−0.041

$$A(x,T_c)=\frac{xNV^2}{2}\frac{\mathrm{Re}\psi(\frac{1}{2}+i\beta|y_0|/2\pi)-\psi(\frac{1}{2})}{y_0[y_0+N\rho V^2(\beta|y_0|/2\pi)\mathrm{Im}\psi'(\frac{1}{2}+i\beta|y_0|/2\pi)]}\ , \tag{3.2}$$

where $y_0=\tilde{E}_0-\epsilon_1$, $\epsilon_1=E_1+\tilde{E}_1-(E_0+\tilde{E}_0)$, and x is impurity concentration. Within the single-impurity approximation, the T_c equation of the system is $\rho[\ln(T_c/T_{c0})+A(x,T_c)]=0$; with x increases, the coupling between two impurities is enhanced, and the relevant term $x^2m[\partial F_{12}(R)/\partial\Delta^2]|_{\Delta^2=0}$ should be added in the T_c equation. We can rewrite (3.1) in the form of

$$T_c=T_{c0}\gamma_1\gamma_2\ , \tag{3.3}$$

where $T_{c0}=1.36$ K, the critical transition temperature of pure superconductor Th, $\gamma_1=\exp[-A(x,T_c)]$, the revision factor of single impurity to T_{c0}, $\gamma_2=\exp\{(-x^2m/\rho)[\partial F_{12}(R)/\partial\Delta^2]|_{\Delta^2=0}\}$, the revision factor of coupling between two impurities to T_{c0}. The numerical results of T_c versus x by solving joint equations (2.7)–(3.2) are shown in Fig. 3, and Table I gives relevant physical parameters.

From Fig. 3, it is identified that, the influence of single nonmagnetic impurity on T_c of the system is significant, while the influence of coupling between nonmagnetic impurities seems not obvious. That means in nonmagnetic mixed-valent rare-earth compound $Th_{1-x}Ce_x$, the T_c depression may be mainly attributed to the mixing interaction between isolated impurity and conducting electron.

The cause of isolated nonmagnetic impurities affecting superconductivity of the system may be the fluctuation of electric charge of $4f$ configuration of Ce: lots of extending electrons nearby the Fermi surface are required to participate in the mixed-valence behavior of $4f$ configuration, thus reducing the numbers of pairable electron; the influence of coupling between nonmagnetic impurities on superconductivity is possibly associated with the fact: the transfer of coupling between nonmagnetic impurities similarly calls for the extending electrons to participate, thus leading to the lesser extending electrons near the Fermi surface.

The numerical results exhibit that pair-breaking effect of the impurity coupling is not strong, and by contrast, the fluctuation of electric charge of $4f$ configuration goes up to a leading factor of depressing the superconductivity of the system. The conclusions are remarkably distinct from ones of magnetic system[1–6] and provide a further cognition of the peculiar nature of nonmagnetic doping.

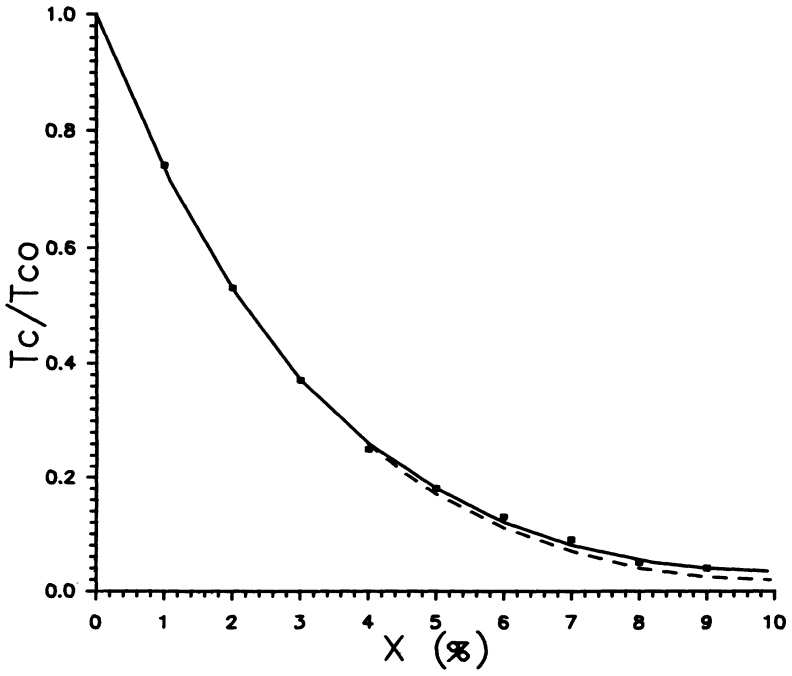

FIG. 3. Critical transition temperature T_c vs impurity content x. The solid curve is the numerical results within single impurity approximation, and the dashed curve is one in which the influence of two impurity coupling is also accounted. The solid marks show the experimental data.

IV. CONCLUSION

On the basis of previous superconductive theory of mixed-valent rare-earth alloys, the mixed Goldstone-Feynman diagrammatic technique is adopted to investigate and compare the influence of both isolated and coupled nonmagnetic mixed-valent impurities on superconductive system $Th_{1-x}Ce_x$, and the results suggest that the mixed-valent fluctuation of the $4f$ configuration play a main role in depressing the superconductivity of the system. The conclusions enable us to acquire a new understanding of the difference between magnetic and nonmagnetic doping.

APPENDIX A: DIAGRAMMATIC METHOD OF TWO IMPURITY COUPLING

The lowest-order impurity-impurity correlation terms appear in the fourth-order perturbation

$$S_{12}^{(4)}=\int_0^\beta d\tau_1\int_0^{\tau_1}d\tau_2\int_0^{\tau_2}d\tau_3\int_0^{\tau_3}d\tau_4\sum_{\{v_i\}}\langle h'_{v_1}(\tau_1)h'_{v_2}(\tau_2)h'_{v_3}(\tau_3)h'_{v_4}(\tau_4)\rangle\ , \tag{A1}$$

where each two $h'_{v_i}(\tau_i)$ vertices locating on the same rare-earth ion can have following three kinds of distributions:

$$(1)v_1=v_2=1\ ,\ \ v_3=v_4=2\ ;\ \ (2)v_1=v_3=1\ ,\ \ v_2=v_4=2\ ;\ \ (3)v_1=v_4=1,\ \ v_2=v_3=2\ .$$

The conduction electrons propagating between $4f$ orbits of the two rare-earth ions are shown in Fig. 1 in terms of the Goldstone-Feynman diagrammatic technique, where two electron lines in each diagram can have independent momentum $\mathbf{k}$, and frequency $i\omega_n$ without violating the conservation law. The rules for writing down the contribution of diagrams in Fig. 1 are the same as those for the fourth-order single-impurity perturbation as stated in Ref. 12 except specifying the site indices $e^{-i\mathbf{k}\cdot\mathbf{R}_v}$ at the corresponding time points.

APPENDIX B: INTERSITE SINGLE ELECTRON'S GREEN'S FUNCTION

Electron of extended states is required to transfer correlation interaction between impurities in superconductive system, and its intersite Green's function is written as[11,12]

$$g_s(\mathbf{R}_1-\mathbf{R}_2,i\omega_n)=\frac{1}{N_s}\sum_{km\sigma}|V_{km\sigma}|^2e^{i\mathbf{k}\cdot(\mathbf{R}_1-\mathbf{R}_2)}\left[\frac{u_k^2}{i\omega_n-E_k}+\frac{v_k^2}{i\omega_n+E_k}\right]\ , \tag{B1}$$

where $V_{km\sigma}$ is mixing interaction strength between extending and $4f$ electrons, $u_k^2=\frac{1}{2}(1+\xi_k/E_k)$, $v_k^2=\frac{1}{2}(1-\xi_k/E_k)$, $E_k=\sqrt{\xi_k^2+\Delta^2}$, ξ_k is the energy of extending electron, and Δ is energy gap. The summation of k can be turned into integral of ξ, thus leading to

$$g_s(x,i\omega_n)=-\frac{\Gamma'}{N_s 2ik_f x}\frac{1}{2i\sqrt{\Delta^2+\omega_n^2}}\int d\xi(i\omega_n+\xi)\left[\frac{-1}{\xi+i\sqrt{\Delta^2+\omega_n^2}}+\frac{1}{\xi-i\sqrt{\Delta^2+\omega_n^2}}\right]$$
$$\times(e^{i(\xi x/V_f)+ik_f x}-e^{-i(\xi x/V_f)-ik_f x})\ , \tag{B2}$$

where $\mathbf{x}=\mathbf{R}_1-\mathbf{R}_2$. If the first term inside square brackets of integrand in formula (B2) takes integral loop of Fig. 4(a), and the second one takes Fig. 4(b), by means of Jordan's lemma and residue theorem, we may obtain

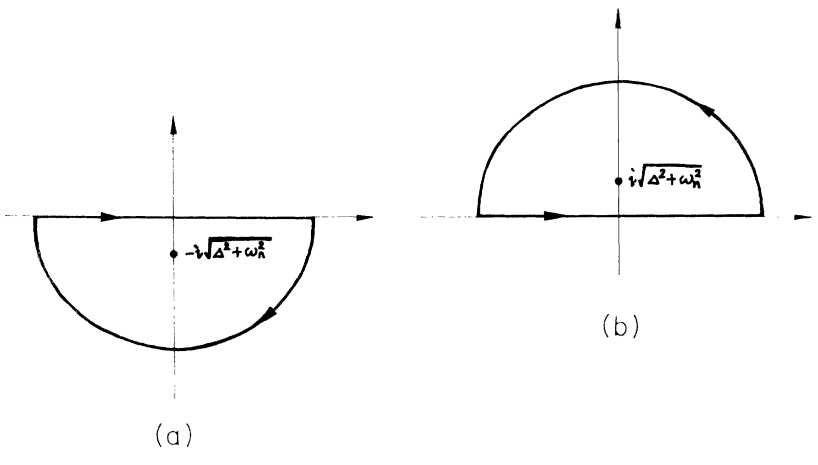

FIG. 4. Two different integral loops of formula (B2).

$$g_s(\mathbf{R}_1-\mathbf{R}_2,i\omega_n)=-\frac{\Gamma}{\alpha}e^{-\frac{\pi\alpha}{y}\sqrt{(n+\frac{1}{2})^2+(\beta\Delta/2\pi)^2}}\frac{\sqrt{(n+\frac{1}{2})^2+(\beta\Delta/2\pi)^2}\cos\alpha+i(n+\frac{1}{2})\sin\alpha}{\sqrt{(n+\frac{1}{2})^2+(\beta\Delta/2\pi)^2}} \tag{B3}$$

in the case, $\alpha=k_f x$, $y=\frac{1}{2}\beta k_f V_f$, V_f is Fermi velocity, $\Gamma=\langle|V_{km\sigma}|^2\rangle$ is orienting average value of $|V_{km\sigma}|^2$ in momentum space near Fermi surface, $\omega_n=(2n+1)\pi/\beta$.

[1]J. Ruvalds and F. S. Liu, Solid State Commun. **39**, 497 (1981).
[2]F. S. Liu and J. Ruvalds, Bull. Am. Phys. Soc. **26**, 344 (1981).
[3]A. A. Abrikosov and L. P. Gorkov, Zh. Eksp. Theor. Fiz. **39**, 1781 (1960) [Sov. Phys. JETP **12**, 1243 (1960)].
[4]F. S. Liu and J. Ruvalds, Physica B **107**, 623 (1981).
[5]J. Kondo, Prog. Theor. Phys. **32**, 37 (1964).
[6]F. S. Liu, Commun. Theor. Phys. **1**, 779 (1982).
[7]M. B. Maple, J. G. Huber, and K. S. Kim, Solid State Commun. **8**, 981 (1970).
[8]J. G. Huber and M. B. Maple, J. Low Temp. Phys. **3**, 537 (1970).
[9]H. Keiter and G. Morandi, Phys. Rep. **109**, 227 (1984).
[10]N. Grewe and H. Keiter, Phys. Rev. B **24**, 4420 (1981).
[11]J. Li, Ph.D. thesis, Manjing University, 1988.
[12]J. Li, C. D. Gong, and A. Holz, Phys. Rev. B **36**, 5230 (1987).
[13]T. V. Ramakrishnan and K. Sur, Phys. Rev. B **26**, 1798 (1982).
[14]F. C. Zhang and T. K. Lee, Phys. Rev. B **28**, 33 (1983).
[15]J. Li and C. D. Gong, Solid State Commun. **62**, 209 (1987).